ELSEVIER

Composite Structures 46 (1999) 115–124

COMPOSITE STRUCTURES

Two shear deformable finite element models for buckling analysis of skew fibre-reinforced composite and sandwich panels

C. Sarath Babu [1], T. Kant *

Indian Institute of Technology Bombay, Powai, Mumbai 400 076, India

Abstract

Two shear deformable finite element models, one based on first-order shear deformation theory and the other based on a higher-order shear deformation theory, are developed for buckling analysis of skew laminated composite and sandwich panels. The procedure involves the development of transformation matrix between global and local degrees of freedom for the nodes lying on the skew edges and suitable transformation of element matrices. The accuracy of the present models is demonstrated by comparing with alternative solutions available in the literature. Extensive numerical results are presented for critical buckling loads of angle-ply and cross-ply skew laminates with various lamination parameters, boundary conditions and width-to-thickness ratios. New results on skew sandwiches, hitherto not reported in the literature, are obtained for different geometric parameters and skew angles.

Keywords: Buckling analysis; Shear deformation theory; Skew laminates; Skew sandwiches

1. Introduction

Fibre-reinforced composite materials due to their high specific strength and stiffness are becoming increasingly used in weight-sensitive applications of aerospace and ship building industries. It is well known that skew or oblique plates made of these materials are important structural components of ship hulls and swept wings of aeroplanes. Buckling is one of the primary modes of failure of these elements when they are subjected to in-plane loads. Thus the stability analysis of such plates is of interest to the designers. The complicating factors in the analysis of skew plates is the non-orthogonal co-ordinate system to be used in the derivation of governing differential equations and finding the solution to these coupled equations. Since there is no exact solution to these equations and associated boundary conditions, numerical methods such as finite element method, finite difference method, Rayleigh–Ritz method, etc. are natural choices upon which one can obtain a conceptual understanding of this important structural mechanics problem.

Considerable amount of literature on the buckling of isotropic and orthotropic skew plates exists. It appears that Anderson [1] is the first person to investigate the buckling problem of an isotropic skew plate. He has used energy method and presented results for different aspect ratios of skew plates. Guest [2] has reported on the buckling of clamped isotropic skew plates subjected to uniaxial compression. Wittrick [3–5] has investigated the buckling problem of rhombic simply supported and clamped plates with a skew angle of 45° under orthogonally compressive and shear loads. He has employed finite difference method in his investigations. Later the stability analysis of isotropic and orthotropic plates are carried out by many researchers [6–14] for various loading and boundary conditions. All of the studies stated above are based on classical plate theory, with the exception of the one by Kitipornchai et al. [14] in which the first-order shear deformation plate theory is adopted for studying the buckling problem of isotropic thick skew plates.

Compared with the literature on isotropic and orthotropic skew plates, very little is reported on buckling analysis of skew composite laminates and sandwiches. Probably the first comprehensive work on the buckling of skew composite laminates is the one by Reddy and Palaninathan [15]. The authors have employed a triangular finite element based on classical laminate plate theory. The results are presented in graphical form. Navin Jaunky et al. [16] have used Rayleigh–Ritz method

* Corresponding author. E-mail: tkant@civil.iitb.ernet.in
[1] E-mail: rssb@civil.iitb.ernet.in

0263-8223/99/$ – see front matter
PII: S0263-8223(99)00039-2

combined with a variational formulation and a first-order shear deformation theory (FSDT), to analyze the buckling of arbitrary quadrilateral anisotropic plates with different boundary conditions. Recently, Wang [17] has employed the B-Spline Rayleigh–Ritz method based on first-order shear deformation theory to study the buckling problem of skew composite laminates. Numerical results are presented for composite laminates subjected to in-plane compressive and shear stresses. But in obtaining the numerical results, standard material properties are not considered as equal shear moduli are taken for the lamina in all the three orthogonal directions. It is observed that buckling analysis of composite laminates with shear deformable finite elements is not attempted so far and also to the best of the authors knowledge, there is no paper in the open literature dealing with the buckling problem of skew sandwich panels.

In the present work, two C° continuous shear deformable finite element formulations are presented for the buckling analysis of skew laminated composites and sandwiches. One of the two models is based on the Reissner–Mindlin first-order theory and the other is based on a higher-order theory developed by Kant and co-workers [18–22]. In the present higher-order formulation, the higher-order terms of displacements and rotations in the Taylor's series expansion of in-plane displacements are taken into account. Accuracy of the present models is verified against the literature values for isotropic and composite skew plates. Some new results are presented for skew composite laminates and sandwiches using standard material properties available in the literature.

2. Theory

2.1. Displacement-models

The two shear deformation theories considered for investigation in the present work are based on the assumption of the displacement fields in the following form.

(a) First-order shear deformation theory (FOST), 5 dof/node

$$\begin{aligned} u(x,y,z) &= u_o(x,y) + z\theta_y(x,y), \\ v(x,y,z) &= v_o(x,y) - z\theta_x(x,y), \\ w(x,y,z) &= w_o(x,y). \end{aligned} \tag{1}$$

(b) Higher-order shear deformation theory (HOST), 9 dof/node

$$\begin{aligned} u(x,y,z) &= u_o(x,y) + z\theta_y(x,y) + z^2u_o^*(x,y) + z^3\theta_y^*(x,y), \\ v(x,y,z) &= v_o(x,y) - z\theta_x(x,y) + z^2v_o^*(x,y) - z^3\theta_x^*(x,y), \\ w(x,y,z) &= w_o(x,y), \end{aligned} \tag{2}$$

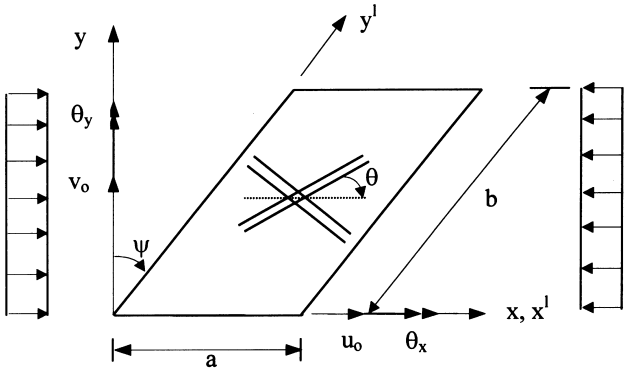

Fig. 1. The geometry of skew laminate with in-plane loading.

where u, v and w define the displacements of any generic point (x, y, z) in the plate space, u_o, v_o and w_o denote the displacements (Fig. 1) of a point (x, y) on the middle plane, θ_x and θ_y are the rotations of normal to middle-plane about x- and y-axes, respectively. The parameters u_o^*, v_o^*, θ_x^* and θ_y^* are higher-order terms in the Taylor's series expansion and are also defined at mid-surface. The continuum displacement vector at the mid-plane can thus be defined as:

$$\begin{aligned} &\text{for FOST} \quad \bar{\boldsymbol{u}} = \{u_o, v_o, w_o, \theta_x, \theta_y\}^{\mathrm{T}}, \\ &\text{for HOST} \quad \bar{\boldsymbol{u}} = \{u_o, v_o, w_o, \theta_x, \theta_y, u_o^*, v_o^*, \theta_x^*, \theta_y^*\}^{\mathrm{T}}. \end{aligned} \tag{3}$$

2.2. Stress–strain relationship

If the transverse stress and strain are neglected, the stress–strain relations for the Lth lamina in the laminate co-ordinates (x, y, z) are written as

$$\begin{Bmatrix} \sigma_x \\ \sigma_y \\ \tau_{xy} \\ \tau_{yz} \\ \tau_{xz} \end{Bmatrix} = \begin{bmatrix} Q_{11} & Q_{12} & Q_{13} & 0 & 0 \\ Q_{12} & Q_{22} & Q_{23} & 0 & 0 \\ Q_{13} & Q_{23} & Q_{33} & 0 & 0 \\ 0 & 0 & 0 & Q_{44} & Q_{45} \\ 0 & 0 & 0 & Q_{45} & Q_{55} \end{bmatrix} \begin{Bmatrix} \varepsilon_x \\ \varepsilon_y \\ \gamma_{xy} \\ \gamma_{yz} \\ \gamma_{xz} \end{Bmatrix} \tag{4}$$

or in short form

$$\boldsymbol{\sigma} = \boldsymbol{Q}\boldsymbol{\varepsilon} \tag{5}$$

in which

$$\begin{aligned} \boldsymbol{\sigma} &= \{\sigma_x \ \sigma_y \ \tau_{xy} \ \tau_{yz} \ \tau_{xz}\}^{\mathrm{T}}, \\ \boldsymbol{\varepsilon} &= \{\varepsilon_x \ \varepsilon_y \ \gamma_{xy} \ \gamma_{yz} \ \gamma_{xz}\}^{\mathrm{T}} \end{aligned} \tag{6}$$

are the stress and the strain vectors, receptively. Q_{ij}'s are the plane stress reduced stiffness coefficients. The transformation of the stresses/strains between the lamina and laminate co-ordinate systems follows the usual stress tensor transformation rule. It may be noted that the formulation given in the rest of the paper is based on HOST and the formulation corresponding to FOST is obtained from that of HOST by truncating the terms corresponding to the higher-order displacement degrees of freedom.

2.3. Strain–displacement relationship

Substituting Eq. (2) into the Green's strain tensor, with $\epsilon_z = 0$, the generalized strain vector components are obtained as:

$$\begin{aligned}
\varepsilon_x &= \varepsilon_x^o + z\chi_x^o + z^2\varepsilon_x^* + z^3\chi_x^* + z^4\varepsilon_x^{**} + z^5\chi_x^{**} + z^6\varepsilon_x^{***},\\
\varepsilon_y &= \varepsilon_y^o + z\chi_y^o + z^2\varepsilon_y^* + z^3\chi_y^* + z^4\varepsilon_y^{**} + z^5\chi_y^{**} + z^6\varepsilon_y^{***},\\
\gamma_{xy} &= \varepsilon_{xy}^o + z\chi_{xy}^o + z^2\varepsilon_{xy}^* + z^3\chi_{xy}^* + z^4\varepsilon_{xy}^{**} + z^5\chi_{xy}^{**} + z^6\varepsilon_{xy}^{***},\\
\gamma_{yz} &= \phi_y^o + z\psi_y^o + z^2\phi_y^* + z^3\psi_y^* + z^4\phi_y^{**} + z^5\psi_y^{**},\\
\gamma_{xz} &= \phi_x^o + z\psi_x^o + z^2\phi_x^* + z^3\psi_x^* + z^4\phi_x^{**} + z^5\psi_x^{**}.
\end{aligned} \tag{7}$$

Note that the five generalized strain components are expressed in terms of 33 strain components ($\bar{\varepsilon}$). Each of the components of strain vector, $\bar{\varepsilon}$ has linear/or non-linear parts which can be expressed in terms of mid-plane displacement components.

The potential energy, Π of the plate can be expressed as

$$\Pi = \frac{1}{2}\int_A \bar{\varepsilon}^{\mathrm{T}}\bar{\sigma}\,\mathrm{d}A - \int_A \bar{u}^{\mathrm{T}}p\,\mathrm{d}A, \tag{8}$$

where, p is the vector of in-plane mechanical loads and

$$\bar{\sigma} = \{N^{\mathrm{T}}\ M^{\mathrm{T}}\ Q^{\mathrm{T}}\}^{\mathrm{T}}. \tag{9}$$

The stress resultants in Eq. (9) are defined as follows:

$$\begin{bmatrix} N_x^o & N_y^o & N_{xy}^o \\ N_x^* & N_y^* & N_{xy}^* \\ N_x^{**} & N_y^{**} & N_{xy}^{**} \\ N_x^{***} & N_y^{***} & N_{xy}^{***} \end{bmatrix} = \sum_{L=1}^{NL}\int_{Z_L}^{Z_{L+1}} \begin{bmatrix} 1 \\ z^2 \\ z^4 \\ z^6 \end{bmatrix} \begin{bmatrix} \sigma_x & \sigma_y & \tau_{xy} \end{bmatrix} \mathrm{d}z, \tag{10}$$

$$\begin{bmatrix} M_x^o & M_y^o & M_{xy}^o \\ M_x^* & M_y^* & M_{xy}^* \\ M_x^{**} & M_y^{**} & M_{xy}^{**} \end{bmatrix} = \sum_{L=1}^{NL}\int_{Z_L}^{Z_{L+1}} \begin{bmatrix} z \\ z^3 \\ z^5 \end{bmatrix} \begin{bmatrix} \sigma_x & \sigma_y & \tau_{xy} \end{bmatrix} \mathrm{d}z, \tag{11}$$

$$\begin{bmatrix} Q_x^o & Q_y^o \\ S_x^o & S_y^o \\ Q_x^* & Q_y^* \\ S_x^* & S_y^* \\ Q_x^{**} & Q_y^{**} \\ S_x^{**} & S_y^{**} \end{bmatrix} = \sum_{L=1}^{NL}\int_{Z_L}^{Z_{L+1}} \begin{bmatrix} 1 \\ z \\ z^2 \\ z^3 \\ z^4 \\ z^5 \end{bmatrix} \begin{bmatrix} \tau_{xz} & \tau_{yz} \end{bmatrix} \mathrm{d}z. \tag{12}$$

After integration, these stress resultants are written in matrix form as

$$\bar{\sigma} = D\bar{\varepsilon}, \tag{13}$$

where,

$$D = \begin{bmatrix} D_M & D_C & 0 \\ D_C^{\mathrm{T}} & D_B & 0 \\ 0 & 0 & D_S \end{bmatrix} \tag{14}$$

in which D_M, D_B, D_c and D_S are the membrane, flexural, membrane–flexural coupling and shear rigidity matrices, respectively.

3. Finite element formulation

Let the region of the plate be divided into finite number of quadrilateral elements. The continuum displacement vector within an element is discretized such that

$$u = \sum_{i=1}^{\mathrm{NN}} N_i u_i, \tag{15}$$

where N_i is the shape function of node i, NN is number of nodes in an element and u_i is the generalized displacement vector corresponding to the ith node of an element. The above relation is expressed in matrix form as

$$u = \bar{N}d, \tag{16}$$

where $\bar{N}$ is element shape function matrix and d is element nodal displacement vector. The components of strain vector, $\bar{\varepsilon}$ can be expressed in terms of nodal displacement vector, d as

$$\bar{\varepsilon} = \left[B_o + \frac{1}{2}B_L\right]d, \tag{17}$$

where, B_o and B_L are linear and non-linear strain–displacement matrices. Substituting for $\bar{\varepsilon}$ from Eq. (17) in Eq. (8) and then minimization of potential energy gives

$$\sum_{i=1}^{NE}\left[K_o^e d + K_g^e d - R\right] = 0, \tag{18}$$

where, NE is the number of elements. K_o^e and K_g^e are the linear and geometric element stiffness matrices and R is the element load vector. These matrices are constructed using the standard procedure [23] as,

$$\begin{aligned}
K_o^e &= \int_A B_o^{\mathrm{T}} D B_o\,\mathrm{d}A,\\
K_g^e d &= \int_A B_L^{\mathrm{T}} S\,\mathrm{d}A,\\
R &= \int_A N^{\mathrm{T}} p\,\mathrm{d}A,
\end{aligned} \tag{19}$$

where, S is the stress resultant matrix.

3.1. Skew boundary transformation

For skew plates supported on two adjacent edges, the edges of the boundary elements may not be parallel to the global axes (x, y, z). In such a situation, it is not possible to specify boundary conditions in terms of the global displacements u_o, v_o, w_o, etc. In order to specify boundary conditions at skew edges, it becomes necessary to use edge displacements u_o^l, v_o^l, w_o^l, etc. in local coordinates (x^l, y^l, z^l) (Fig. 1). It is thus required to transform the element matrices corresponding to global axes to local edge axes with respect to which the boun-

dary conditions can be conveniently specified. The relation between the global and local degrees of freedom of a node can be obtained through the simple transformation rules [23,24] and the same can be expressed as

$$\boldsymbol{d}_i = \boldsymbol{L}_g \boldsymbol{d}_i^l \tag{20}$$

in which $\boldsymbol{d}_i$ and $\boldsymbol{d}_i^l$ are the generalized displacement vectors in the global and local edge coordinate system, respectively of node i and they are defined as

$$\boldsymbol{d}_i = \left\{u_o, v_o, w_o, \theta_x, \theta_y, u_o^*, v_o^*, \theta_x^*, \theta_y^*\right\}^{\mathrm{T}},$$

$$\boldsymbol{d}_i^l = \left\{u_o^l, v_o^l, w_o^l, \theta_x^l, \theta_y^l, u_o^{*^1}, v_o^{*^1}, \theta_x^{*^1}, \theta_y^{*^1}\right\}^{\mathrm{T}}. \tag{21}$$

The node transformation matrix for a node i, on the skew boundary is

$$\boldsymbol{L}_g = \begin{bmatrix} c & s & 0 & 0 & 0 & 0 & 0 & 0 & 0 \\ -s & c & 0 & 0 & 0 & 0 & 0 & 0 & 0 \\ 0 & 0 & 1 & 0 & 0 & 0 & 0 & 0 & 0 \\ 0 & 0 & 0 & c & s & 0 & 0 & 0 & 0 \\ 0 & 0 & 0 & -s & c & 0 & 0 & 0 & 0 \\ 0 & 0 & 0 & 0 & 0 & c & s & 0 & 0 \\ 0 & 0 & 0 & 0 & 0 & -s & c & 0 & 0 \\ 0 & 0 & 0 & 0 & 0 & 0 & 0 & c & s \\ 0 & 0 & 0 & 0 & 0 & 0 & 0 & -s & c \end{bmatrix} \tag{22}$$

in which $c = \cos(\Psi)$ and $s = \sin(\Psi)$, where Ψ is skew angle of the plate. It may be noted that for nodes which are not on lying on skew edges, the node transformation matrix consists of all elements being zero except the principal diagonal elements which are equal to unity. Thus for the complete element, the element transformation matrix is written as,

$$\boldsymbol{T}_e = \begin{bmatrix} \boldsymbol{L}_g & 0 & 0 & \dots \\ 0 & \boldsymbol{L}_g & 0 & \\ 0 & 0 & \boldsymbol{L}_g & \\ \vdots & & & \end{bmatrix} \tag{23}$$

in which the number of $\boldsymbol{L}_g$ matrices are equal to the number of nodes in the element. For those elements whose nodes are on the skew edges, the element matrices are transformed to the local axes using the element transformation matrix, T_e. After the transformation of element matrices, Eq. (18) is expressed as

$$\sum_{i=1}^{NE}\left[\boldsymbol{K}_o^l \boldsymbol{d} + \boldsymbol{K}_g^l \boldsymbol{d} - \boldsymbol{R}^l\right] = 0, \tag{24}$$

where

$$\boldsymbol{K}_o^l = \boldsymbol{T}_e^{\mathrm{T}} \boldsymbol{K}_o^e \boldsymbol{T}_e, \qquad \boldsymbol{K}_g^1 = \boldsymbol{T}_e^{\mathrm{T}} \boldsymbol{K}_g^e \boldsymbol{T}_e \qquad \text{and} \qquad \boldsymbol{R}^1 = \boldsymbol{T}_e^{\mathrm{T}} \boldsymbol{R}. \tag{25}$$

Eq. (24) is solved in two stages. In the first stage, the geometric stiffness matrix is neglected and stress analysis is performed to determine the stress resultants. These stress resultants are used to compute geometric stiffness matrix in the second stage and then the stability problem is solved as an eigenvalue problem as

$$\left[\boldsymbol{K}_o + \lambda \boldsymbol{K}_g\right]\delta \boldsymbol{d} = 0 \tag{26}$$

in which, $\boldsymbol{K}_o$ and $\boldsymbol{K}_g$ are the assembled linear stiffness and geometric stiffness matrices, respectively. The subspace iteration method [25] is used to solve the eigenvalue problem.

4. Numerical results and discussion

Computer programs are developed based on the foregoing finite element models to solve a number of numerical examples on buckling of skew composite laminates and sandwiches. A 6×6 skew mesh of 16-noded element is used in computations. This scheme is arrived at on the basis of convergence study in which the critical buckling load converges monotonically from a higher value. The details of the convergence study is not presented here for the sake of brevity. The selective integration scheme, namely 4×4 Gauss–Legendre for membrane, flexure, membrane–flexure and 3×3 for shear contributions of energy, is used for thin laminates (a/h > 20, h – thickness of plate) and a full (4×4) integration scheme is used for thick laminates. All the laminates considered are assumed to have an aspect ratio of $a/b = 1$, though the general case $a \neq b$ can also be studied without any difficulty. In all the computations of FOST model, a shear correction factor of 5/6 is used.

The accuracy of the present finite element formulations is evaluated first for isotropic and composite skew plates with the available literature results. Subsequently, some new results are presented for laminated composite and sandwich skew plates subjected to uniaxial compression. The buckling loads are expressed in terms of non-dimensional parameter, $\lambda_U = \bar{N}_x b^2/E_2 h^3$. Two types of simply supported boundary conditions, SS1 and SS2 are used (Table 1). The notations used in the tables below for boundary conditions SSSS and CCCC represent all edges are simply supported and clamped, respectively. The following sets of material properties are used in numerical studies.

Material 1	Material 2
$E_1/E_2 = 40$	$E_1/E_2 = 40$
$G_{12}/E_2 = G_{13}/E_2 = 0.5$,	$G_{12}/E_2 = G_{13}/E_2 = 0.6$,
$G_{23}/E_2 = 0.2$	$G_{23}/E_2 = 0.5$
$v_{12} = v_{23} = v_{13} = 0.25$	$v_{12} = v_{23} = v_{13} = 0.25$

Material 3 (sandwich)

Face sheets

$$E_1/E_2 = 19, \quad G_{12}/E_2 = G_{13}/E_2 = 0.52, \quad G_{23}/E_2 = 0.338,$$

$$v_{12} = v_{13} = 0.32, \qquad v_{23} = 0.49.$$

Core

Table 1
Details of boundary conditions for laminated skew plates and sandwiches

Boundary	Model	Simply Supported		Fixed
		SS1	SS2	
$x^1 = 0, a$	FOST	$v_o^1 = w_o^1 = 0, \theta_x^1 = 0$	$u_o^1 = w_o^1 = 0, \theta_x^1 = 0$	$u_o^1 = v_o^1 = w_o^1 = 0, \theta_x^1 = \theta_y^1 = 0$
	HOST	$v_o^1 = w_o^1 = 0, \theta_x^1 = v_o^{*1} = 0, \theta_x^{*1} = 0$	$u_o^1 = w_o^1 = 0, \theta_x^1 = u_o^{*1} = 0, \theta_x^{*1} = 0$	$u_o^1 = v_o^1 = w_o^1 = 0, \theta_x^1 = \theta_y^1 = u_o^{*1} = 0, v_o^{*1} = \theta_x^{*1} = \theta_y^{*1} = 0$
$y^1 = 0, b$	FOST	$u_o^1 = w_o^1 = 0, \theta_y^1 = 0$	$v_o^1 = w_o^1 = 0, \theta_y^1 = 0$	$u_o^1 = v_o^1 = w_o^1 = 0, \theta_x^1 = \theta_y^1 = 0$
	HOST	$u_o^1 = w_o^1 = 0, \theta_y^1 = u_o^{*1} = 0, \theta_y^{*1} = 0$	$v_o^1 = w_o^1 = 0, \theta_y^1 = v_o^{*1} = 0, \theta_y^{*1} = 0$	$u_o^1 = v_o^1 = w_o^1 = 0, \theta_x^1 = \theta_y^1 = u_o^{*1} = 0, v_o^{*1} = \theta_x^{*1} = \theta_y^{*1} = 0$

$E_1/E_2^f = 3.2 \times 10^{-5}$, $E_2/E_2^f = 2.9 \times 10^{-5}$,
$E_3/E_2^f = 0.4$, $G_{12}/E_2^f = 2.4 \times 10^{-3}$,
$G_{13}/E_2^f = 7.9 \times 10^{-2}$, $G_{23}/E_2^f = 6.6 \times 10^{-2}$,
$v_{12} = 0.99$, $v_{13} = v_{23} = 3 \times 10^{-5}$
in which E_2^f refers to that of face sheets.

4.1. Isotropic skew plates

Critical buckling loads of isotropic thin ($a/h = 1000$) and thick ($a/h = 10$) skew plates subjected to uniaxial compression are determined for both simply supported and clamped boundary conditions. The buckling loads are evaluated in non-dimensional form, expressed as $K_{cr} = \bar{N}_x b^2/(\pi^2 D)$, where $\bar{N}_x$ is the critical buckling load, $D = Eh^3/[12(1 - v^2)]$ and E is the Young's modulus. Poisson's ratio, v is taken as 0.3. The results are presented in Table 2 along with the other literature results for four different values of $\Psi = 0°$, 15°, 30° and 45°. It is to be noted that the solutions of the present FOST and HOST models match well with the literature results.

4.2. Angle-ply skew laminates

Angle-ply skew laminates with symmetric and antisymmetric lay-ups are considered in this section. Results are presented showing the effects of skew angle, various lamination parameters such as number of layers, fibre-orientation angle and boundary conditions on critical buckling load.

4.2.1. Antisymmetric laminates

Simply supported (SS1) and clamped skew laminates [(45/-45/...)] having $a/h = 10$ are analyzed. Plates with 2, 4, 12 layer lay-ups are considered. The material properties of each layer are $E_1/E_3 = 40$, $E_2 = E_3$, $G_{12} = G_{23} = G_{13} = 0.5E_3$, $v_{12} = v_{23} = v_{13} = 0.25$. The solutions of present formulations along with those obtained by Wang [17] using Rayleigh–Ritz method (RRM) with FSDT is given in Table 3. It is to be noted that the results of FOST and RRM match well for all the lay-ups considered. But the results of these two models are higher in comparison to that of HOST for two and four layer laminates. The differences may be due to the assumption of an arbitrary value of 5/6 for shear

Table 2
Buckling load parameter, K_{cr} for isotropic skew plates

Plate type	Support conditions	Researchers	Skew angle (Ψ)			
			0	15	30	45
Thin	SSSS	Durvasula [7]	4.00	4.48	6.41	12.30
		Tham and Szeto [12]	4.00	4.38	5.93	10.36
		Wang [17]	4.00	4.39	5.90	10.12
		HOST	4.00	4.40	5.92	10.23
		FOST	4.00	4.40	5.92	10.23
	CCCC	Argyris [11]	10.15	–	13.76	20.44
		Durvasula [6]	10.08	10.87	13.58	20.44
		Tham and Szeto [12]	10.08	10.84	13.60	20.60
		Wang [17]	10.07	10.83	13.54	20.12
		HOST	10.07	10.84	13.54	20.12
		FOST	10.07	10.84	13.54	20.12
Thick	SSSS	Wang [17]	3.73	4.08	5.35	8.52
		Kitipornchai et al. [14]	3.79	4.14	5.46	8.80
		HOST	3.73	4.08	5.38	8.65
		FOST	3.73	4.08	5.38	8.65
	CCCC	Wang [17]	8.02	8.47	9.96	13.02
		Kitipornchai et al. [14]	8.29	8.77	10.38	13.69
		HOST	8.04	8.49	9.99	13.11
		FOST	8.03	8.48	9.97	13.05

Table 3
Buckling load parameter (λ_U/π^2) for skew antisymmetric angle-ply laminates

NL	Skew angle (Ψ)								
	15			30			45		
	HOST	FOST	RRM [17]	HOST	FOST	RRM	HOST	FOST	RRM
(a) simply supported									
2	1.7759	1.9187	1.9021	2.0406	2.1884	2.1707	2.6099	2.7515	2.7022
4	2.7416	3.0350	3.0314	3.0195	3.3449	3.3240	3.4861	3.7921	3.8204
12	3.2273	3.2299	3.2507	3.5193	3.5216	3.5251	3.9795	3.9370	3.9791
(b) clamped									
2	2.1604	2.3089	2.2972	2.4092	2.5724	2.5570	2.8794	3.0263	3.0436
4	3.0193	3.3256	3.3238	3.2072	3.5327	3.5332	3.5647	3.8596	3.9390
12	3.5098	3.4808	3.4975	3.7185	3.6708	3.6880	4.0462	3.9650	4.0718

correction factors which depend on several factors such as number of layers, lamination angle etc. In case of laminates with 12 layers, i.e., when the behaviour of the laminate tends to be orthotropic, a close agreement exists between the present results and infinite layer solution of RRM.

Figs. 2 and 3 show the variation of buckling load parameter, λ_U with fibre-orientation angle and number of layers for simply supported (SS2) thin ($a/h = 1000$) and thick ($a/h = 10$) skew laminates (material 1). These results are obtained with FOST and HOST models for thin and thick plates, respectively. It is observed that the present thin plate solutions has shown good agreement with the finite element solutions of Krishna Reddy and Palaninathan [15] for all values of $\theta < 60°$ in which the buckling mode shape is ($m = 1$, $n = 1$). For $\theta \geqslant 60°$, when mode shape changes from (1,1) to (2,1) or (3,1), their results are higher to the present results and the differences increase with increasing skew angles. The reason for this may be due to employing a coarse mesh of 4×4 in their numerical computations. The authors have determined buckling load ratios, $a_1 = \{(\lambda_U)_{\theta=0}/(\lambda_U)_{\theta=90}\}$ and it is shown that for plates with $\Psi = 45°$, $a_1 = 0.787$. The value of a_1 obtained based on

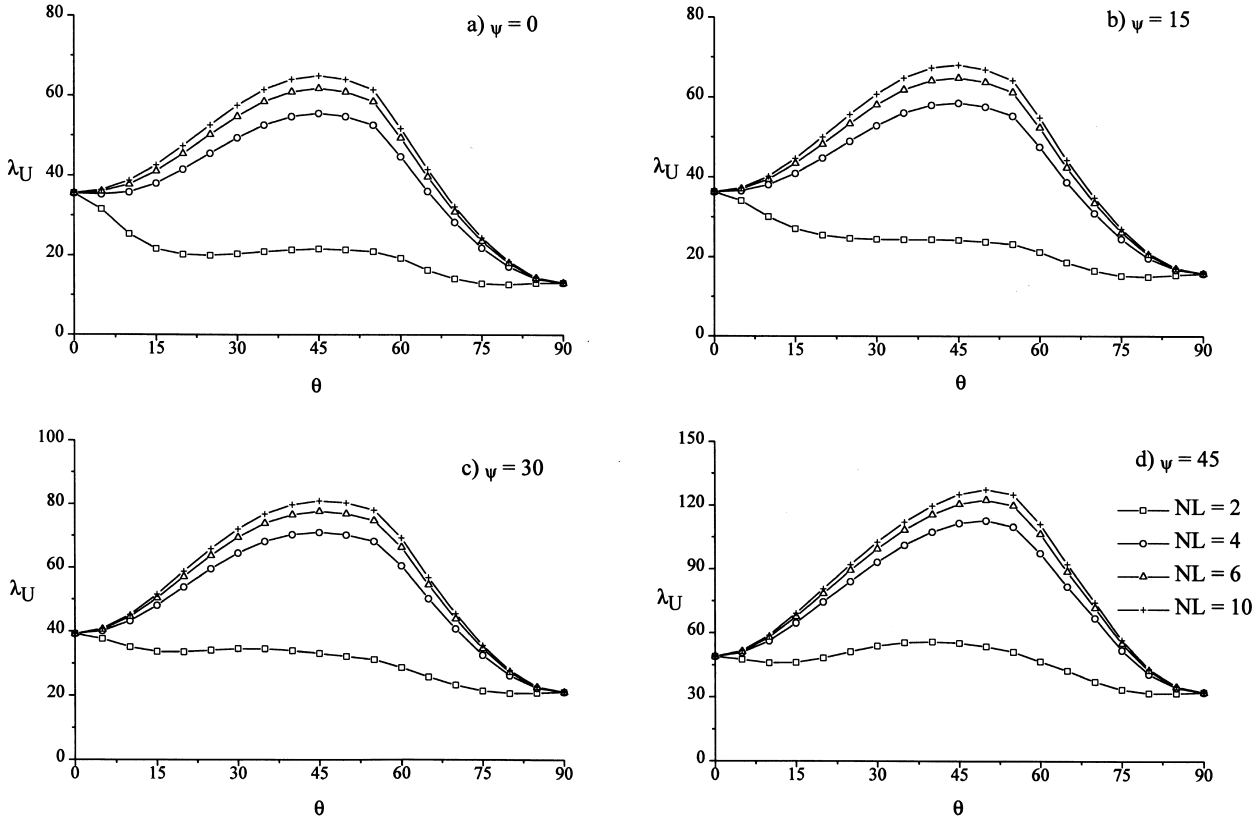

Fig. 2. Uniaxial buckling loads for simply supported antisymmetric angle-ply skew laminates ($a/b = 1, a/h = 1000$).

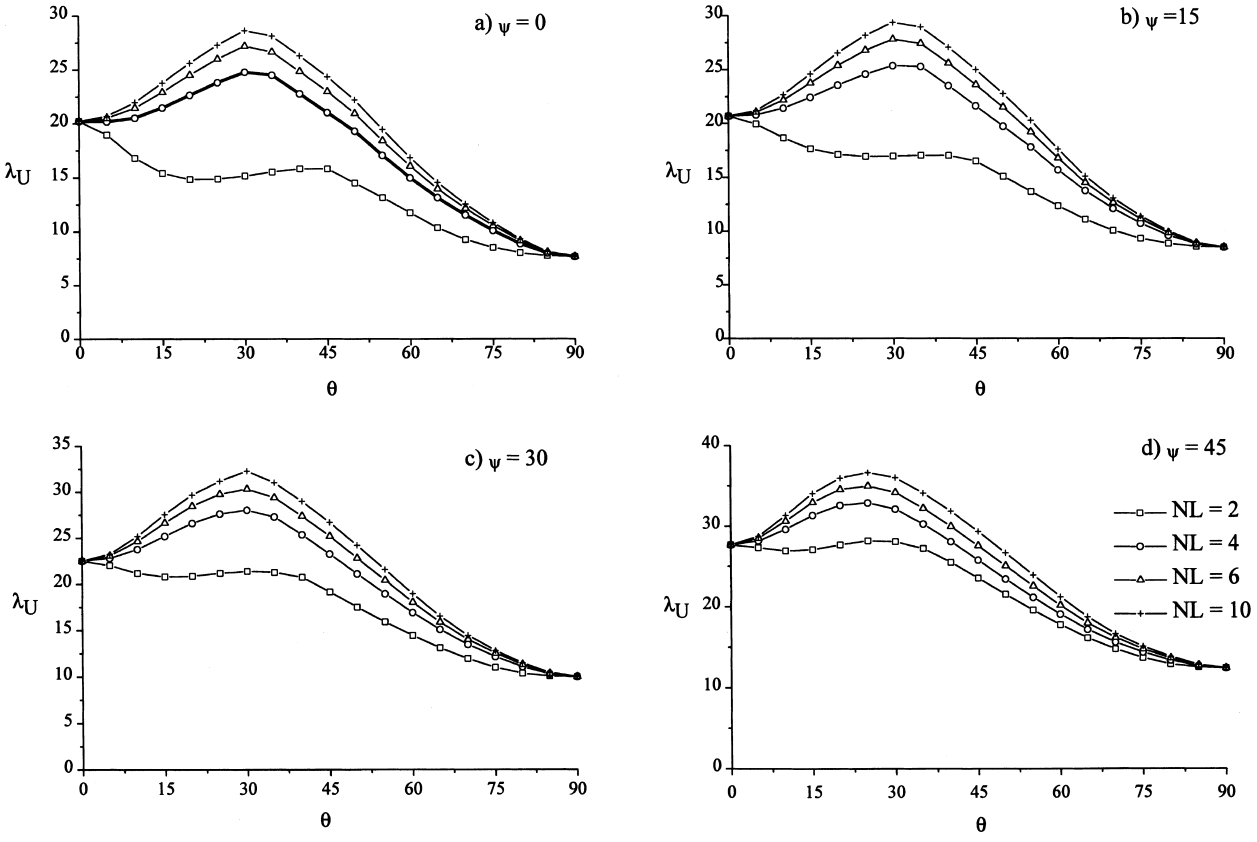

Fig. 3. Uniaxial buckling loads for simply supported antisymmetric angle-ply skew laminates ($a/b = 1, a/h = 10$).

the present fully converged buckling loads is 1.52. Thus their observation that skew plates with $\Psi = 45°$ has more buckling strength for 90° lamination than for 0° lamination is not correct and the present results clearly establish that skew plates with $\theta = 0°$ fibre-orientation has significantly higher buckling strength than the ones with $\theta = 90°$ fibre-orientation.

It may be noticed that the buckling load factor of both thin and thick skew laminates increases with the increase in number of layers and eventually, the behaviour of laminates tend to be that of orthotropic homogeneous one for very large layers. The buckling load factor of both thin and thick laminates increases as the skew angle of the laminates increases. But the increase is small in thick plates because of the effect of large transverse shear flexibility. The attractive feature of composite laminates, the fibre-orientation effect (increase in λ_U with θ) is seen to increase with the increase in skew angle for thin laminates. However, in case of thick laminates, this effect is more or less remain same for plates with $\Psi = 0°$, 15°, 30° and then decreases for plates with $\Psi = 45°$.

4.2.2. Symmetric laminates

Critical buckling loads of 3-layer $(\theta/-\theta/\theta)$ and 7-layer $[(\theta/-\theta/\theta/-\bar{\theta})_s]$ regular symmetric skew laminates (material 1) having $a/h = 10$ are determined. The numerical results are presented in Tables 4 and 5 for the respective SSSS (SS2)and CCCC laminates for four fibre-orientations, i. e., $\theta = 0°$, 15°, 30° and 45°. No direct comparative solutions are available in the literature. It is observed that FOST results are slightly lower than HOST results for $\theta = 0°$. For other values of θ, FOST results are higher than HOST results. The differences between the FOST and HOST solutions are small for 7-layer laminates. In general bucking load factors increase with the skew angle with the exception of 3-layer laminate with $\theta = 15°$, in which the buckling load initially decreases as Ψ increases from 0° to 15° and thereafter increases with Ψ. The effect of boundary conditions is seen to reduce as the skew angle increases.

4.3. Cross-ply skew laminates

Only symmetric laminates are considered and antisymmetric laminates are not considered as true bifurcation buckling can not physically occur for such laminates. Symmetric skew laminates (material 2) having $a/h = 10$ and made up of 3, 5 and 9-layer lay-ups are analyzed. The outer layers of all the laminates are of zero degree lamina and the thickness of middle layer is twice that of other layers. Numerical results are recorded in Table 6 for both SSSS (SS1) and CCCC support conditions. The solutions of both FOST and

Table 4
Buckling load parameter, λ_U for SSSS skew composite laminates with symmetric angle-ply lay-ups

NL	θ	Skew angle (Ψ)							
		0		15		30		45	
		HOST	FOST	HOST	FOST	HOST	FOST	HOST	FOST
3	0	20.227	20.116	20.684	20.569	22.499	22.365	27.671	27.450
	15	19.170	19.559	18.506	18.882	20.103	20.558	26.430	27.279
	30	18.346	19.278	18.832	19.893	21.552	22.681	24.304	25.748
	45	16.226	17.053	16.201	17.054	16.752	17.755	20.099	21.303
7	0	20.227	20.116	20.684	20.569	22.499	22.365	27.671	27.450
	15	22.832	23.353	23.086	23.733	25.594	26.316	32.110	32.749
	30	26.516	27.931	27.457	28.838	30.226	31.240	33.288	34.169
	45	22.875	24.168	23.399	24.188	24.980	25.738	27.333	27.985

Table 5
Buckling load parameter, λ_U for CCCC skew composite laminates with symmetric angle-ply lay-ups

NL	θ	Skew angle (Ψ)							
		0		15		30		45	
		HOST	FOST	HOST	FOST	HOST	FOST	HOST	FOST
3	0	35.115	34.254	35.521	34.592	36.921	35.757	39.888	38.195
	15	28.789	29.054	28.506	28.968	29.610	30.161	32.737	33.326
	30	22.835	23.800	22.958	24.007	24.314	25.529	27.039	28.463
	45	17.828	18.635	17.956	18.887	19.293	20.330	22.115	22.989
7	0	35.115	34.254	35.521	34.592	36.921	35.757	39.888	38.195
	15	33.704	33.813	33.826	34.108	35.206	35.553	37.911	38.185
	30	30.638	31.136	30.854	31.528	31.992	32.844	34.042	34.712
	45	24.432	25.069	24.876	25.426	25.940	26.534	27.738	28.200

HOST match well for simply supported skew laminates. For clamped plates, the results of FOST are slightly lower to that of HOST with a maximum deviation of about 5%.

Fig. 4(a) and (b) show the effect of span to thickness ratio on the critical buckling load of 3-layer skew laminate for SSSS and CCCC support conditions, respectively. The critical buckling load parameter decreases, i.e. the effect of transverse shear deformation increases with the increase of thickness. It is seen that the effect of transverse shear deformation increases with the skew angle for both SSSS and CCCC laminates. The increase is more pronounced in CCCC laminate. The effect of boundary conditions and skew angle decreases as the thickness of laminate increases.

Table 6
Buckling load parameter, λ_U for simply supported and clamped skew composite laminates with symmetric cross-ply lay-ups

Support conditions	Ψ	Theory	NL		
			3	5	9
SSSS	0	HOST	22.965	24.865	25.416
		FOST	23.084	24.821	25.378
	15	HOST	24.267	26.779	27.642
		FOST	24.505	26.803	27.607
	30	HOST	29.237	33.648	35.373
		FOST	29.887	33.865	35.195
	45	HOST	39.714	45.516	46.033
		FOST	40.573	45.754	46.585
CCCC	0	HOST	40.749	43.525	42.877
		FOST	40.069	41.374	40.689
	15	HOST	41.216	44.166	43.559
		FOST	40.691	42.073	41.375
	30	HOST	42.943	45.993	45.503
		FOST	42.454	43.833	43.163
	45	HOST	46.155	48.933	48.681
		FOST	45.310	46.744	46.097

4.4. Skew sandwiches

Sandwich skew panels comprising of cross-ply composite face sheets and honeycomb central core (material 3) are considered here. The fibre-orientation of the layers of the bottom face sheet is $[0/90]_5$, with the fibres of the bottom layer making 0° with x-axis. The layers of the top face sheet are positioned, with respect to the sandwich middle surface ($z=0$), so as to make the sandwich lamination orientation symmetric. Numerical results are presented in Table 7 for simply supported (SS1) panels for four different values of $\Psi=0°$, 15°, 30° and 45°. Two parameters, a/h and h_f/h are varied, where h_f is thickness of face sheet. For validation of the present models, the 3-D elasticity solution results [26] are also given for panels with $\Psi=0°$. It may be noted that the results of HOST match well with 3-D elasticity

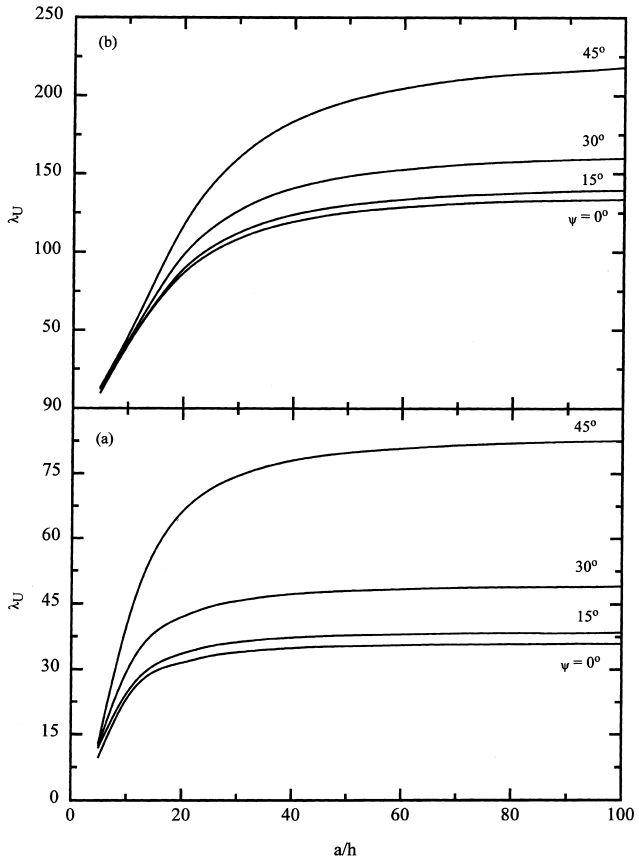

Fig. 4. Effect of thickness ratio on buckling load of symmetric cross-ply $[(0/90)_s]$ skew laminates: (a) SSSS; (b) CCCC.

solution for all values of h_f/h whereas FOST overestimates the buckling load with significant margin at higher values of h_f/h. In case of skew panels, HOST and FOST show good agreement with each other for sandwiches with very thin face sheets ($h_f/h = 0.025$). But for sandwiches with $h_f/h \geqslant 0.050$, FOST results are on the higher side to that of HOST and the differences increase with increasing h_f/h and Ψ. For panels with $\Psi = 45°$ and $h_f/h = 0.15$, FOST in comparison to HOST overestimates the buckling load by as much as 48% when $a/h = 10$ and by about 23% when $a/h = 20$.

5. Concluding remarks

Two C° isoparametric finite element formulations, one based on first-order shear deformation theory and the other based on a higher-order shear deformation theory, are presented for buckling analysis skew fibre-reinforced composite and sandwich laminates. By the use of transformation matrices for the nodes lying on the skew edges, the general finite element formulation in orthogonal co-ordinates is extended to the analysis of skew plates. The accuracy of the present formulations is evaluated with the available results in the literature. Numerical results are presented for isotropic, anisotropic and sandwich plates with skew geometries.

The sensitivity of the buckling coefficient to the variations in skew angle, width-to-thickness ratio and boundary conditions is studied. The influence of skew angle on buckling coefficient is more pronounced as the skew angle increases and this influence is more significant in thin plates than in thick plates. In thick laminates, the transverse shear deformation effect is significant and this effect increases with increasing skew angle. The results also show that in case of composite laminates the differences in predictions of first-order

Table 7
Buckling load parameter, λ_U for simply supported skew sandwiches with composite cross-ply face sheets

a/h	Ψ	Theory	h_f/h				
			0.025	0.050	0.075	0.100	0.150
20	0	3-D elasticity [26]	2.5534	4.6460	6.4401	7.9352	–
		HOST	2.5536	4.6756	6.4528	7.9512	10.3405
		FOST	2.5437	4.7128	6.6156	8.2984	11.1017
	15	HOST	2.9241	5.3212	7.3053	8.9628	11.6015
		FOST	2.9200	5.3817	7.5319	9.4311	12.5977
	30	HOST	4.3601	7.7733	10.4931	12.6998	16.1573
		FOST	4.3538	7.9078	10.9744	13.6732	18.1833
	45	HOST	7.7560	13.1498	17.0275	19.9271	24.3272
		FOST	7.7813	13.6269	18.5161	22.7913	30.0425
10	0	3-D elasticity	2.2081	3.7385	4.8307	5.6721	–
		HOST	2.2122	3.7499	4.8643	5.7100	7.0095
		FOST	2.2043	3.8662	5.2650	6.4930	8.5749
	15	HOST	2.4596	4.1129	5.3038	6.1912	7.5452
		FOST	2.4707	4.2860	5.8043	7.1361	9.4036
	30	HOST	3.4292	5.4380	6.7133	7.4876	8.5624
		FOST	3.4336	5.7238	7.5725	9.1767	11.9388
	45	HOST	5.1826	7.1102	7.9533	8.4699	9.5719
		FOST	5.1083	7.6524	9.5314	11.1782	14.1729

theory and higher-order theory are small. However, for sandwiches the first-order theory in comparison to higher-order theory overestimates the buckling load with significant margin and the differences increase as the skew angle increases. It is believed that the present results on skew sandwiches are first of its kind and it is hoped that these results may serve as benchmark solutions for other researchers to validate their numerical techniques.

References

[1] Anderson RA. Charts giving critical compressive stress of continuous flat sheet divided in to parallelogram shaped panels. NACA, TN 2392, 1951.

[2] Guest J. Compressive buckling of a parallelogram plate simply supported along all four edges, Rep. SM 199. Melbourne: Aeronautical Research Laboratories, 1952.

[3] Wittrick WH. Buckling of oblique plates with clamped edges under uniform compression. Aeronautical Quart 1952; 4(2):151–63.

[4] Wittrick WH. Buckling of oblique plates with uniform shear. Aeronautical Quart 1954;5(1):39–51.

[5] Wittrick WH. On the buckling of oblique plates in shear. Aircraft Eng 1956;28:25–27.

[6] Durvasula S. Buckling of clamped skew plates. AIAA J 1970;8(1):178–81.

[7] Durvasula S. Buckling of simply supported skew plates. ASCE J Eng Mech 1971;97(3):967–79.

[8] Srinivasan RS, Ramachandran SV. Stability of generally orthotropic skew plate. ASCE J Eng Mech 1976;102(3):569–72.

[9] Kennedy JB, Prabhakara MK. Buckling of simply supported orthotropic skew plates. Aeronautical Quart. 1978; 29(3):161–74.

[10] Kennedy JB, Prabhakara MK. Combined load buckling of orthotropic skew plates. ASCE J Eng Mech 1979;105(1):569–72.

[11] Argyris JH. Continua and discontinua (An apercu of recent developments of the matrix displacement method). In: Proceedings of the Matrix Methods in Structural Mechanics Ohio: Wright Air Development Center, 1966:11–190.

[12] Tham LG, Szeto HY. Buckling analysis of arbitrarily shaped plates by spline finite strip method. Comput and Structures 1990;36(4):729–35.

[13] Wang CM, Liew KM, Alwis WA. Buckling of skew plates and corner condition for simply supported edges. ASCE J Eng Mech 1992;118(4):651–62.

[14] Kitipornchai S, Xiang Y, Wang CM, Liew KM. Buckling of thick skew plates. Res Rep Ser 1992;136:1–20.

[15] Reddy ARK, Palaninathan R. Buckling of laminated skew plates. Thin-Walled Structures 1995;22:241–59.

[16] Navin Jaunky, Knight Jr NF, Ambur DR. Buckling of arbitrary quadrilateral anisotropic plates. AIAA J 1995;33(5):938–44.

[17] Wang S. Buckling analysis of skew fibre-reinforced composite laminates based on first-order shear deformation plate theory. Composite Structures 1997;37(1):5–19.

[18] Kant T. Numerical analysis of thick plates. Comput Meth Appl Mech Eng 1982;31(1):1–18.

[19] Kant T, Owen DRJ, Zienkiewicz OC. A refined higher-order C° plate bending element. Computers and Structures 1982;15(2):177–83.

[20] Kant T, Pandya BN. A simple finite element formulation of a higher-order theory for unsymmetrically laminated composite plates. Composite Structures 1988;9:215–46.

[21] Kant T, Mallikarjuna. A higher-order theory for free vibration of unsymmetrically laminated composite and sandwich plates – finite element evaluations. Comput and Structures 1989;32(5):1125–32.

[22] Kant T, Mallikarjuna. Vibration of unsymmetrically laminated plates analyzed by using a higher-order theory with a C° finite element formulation. J Sound and Vibration 1989;134(1):1–16.

[23] Zienkiewicz OC, Taylor RL. The Finite Element Method vol. 1, 4th ed. Singapore: McGraw-Hill, 1989.

[24] Butalia TS, Kant T, Dixit VD. Performance of heterosis element for bending of skew rhombic plates. Comput and Structures 1990;34(1):23–49.

[25] Bathe KJ. Finite Element Procedures, 1st ed. Englewood Cliffs: Prentice-Hall, 1996.

[26] Noor AK, Peters JM, Burton WS. Three-dimensional solutions for initially stressed structural sandwiches. ASCE J Eng Mech 1994;120(2):284–303.